

Quantitative Assessment of In Vivo HIV Protease Activity Using Genetically Engineered QD-Based FRET Probes

Lakshmi N. Cella,¹ Payal Biswas,¹ Marylynn V. Yates,² Ashok Mulchandani,¹ Wilfred Chen³

¹Department of Chemical and Environmental Engineering, University of California, Riverside, California

²Department of Environmental Sciences, University of California, Riverside, California

³Department of Chemical and Biomolecular Engineering, University of Delaware, Newark, Delaware 19716; telephone: +1-302-831-6327; fax: 302-831-1048; e-mail: wilfred@udel.edu

ABSTRACT: HIV protease plays a central role in its life cycle leading to release of functional viral particles. It has been successfully used as a therapeutic target to block HIV infection. Several protease inhibitors (PIs) are currently being employed as a part of anti-HIV therapy. However, the constant genetic drift in the virus leads to accumulation of mutations in both cleavage site and the protease, resulting in resistance and failure of therapy. We reported the use of a quantum dot (QD)-based protein probe for the in vivo monitoring of HIV-1 protease activity based on fluorescence resonance energy transfer. In the current study, we demonstrate the utility of this approach by quantifying the in vivo cleavage rates of three known protease and cleavage site mutations in the presence or absence of different PIs. The changes in IC₅₀ values for the different PIs were similar to that observed in patients, validating our assay as a rapid platform for PI screening.

Biotechnol. Bioeng. 2014;111: 1082–1087.

© 2014 Wiley Periodicals, Inc.

KEYWORDS: HIV protease; quantum dots; FRET; in vivo kinetics; viral detection

Introduction

Since the early 1980s, millions of individuals throughout the world have been infected with human immunodeficiency virus (HIV; UNAIDS, 2010). Many biochemical events critical to HIV replication have been used for therapeutic intervention (Brik and Wong, 2003; Dayam and Neamati,

2003; Imamichi, 2004). Among them, the HIV protease (HIV-1 Pr), which is essential for releasing the individual protein subunits from the translated polyproteins (Navia et al., 1989), was quickly recognized as an important target. Although many protease inhibitors (PIs) are currently approved for patient treatment (Craig et al., 1991; Robinson et al., 2000; Sham et al., 1998; Vacca et al., 1994; Virgil, 2010), over 50% of the patients who achieve initial viral suppression with PIs will eventually experience treatment failure because of the rapid emergence of drug-resistant HIV-1 variants (Grabar et al., 2000). The resistance occurs due to multiple mutations in both the protease and the cleavage sites that alter PI binding, resulting in a loss of efficacy (Ali et al., 2010; Menéndez-Arias, 2010; Wensing et al., 2010). Continual success in future treatments depends on the development of new antiviral agents that maintain efficacy against drug-resistant viral strains.

High throughput assays have been developed to identify new HIV PIs, and the majority of them are in vitro assays based on purified enzymes and peptido-mimetic substrates (De Clercq, 2002; Randolph and DeGoey, 2004). Cell-based assays are considered a better alternative since they can be used to identify PIs with different modes of action under the native intracellular environment along with their preliminary toxicity profile (Cheng et al., 2006; Fuse et al., 2006; Roh et al., 2010). Unfortunately, establishment of a different genetically modified cell line for all the mutated protease and cleavage site combinations remains a formidable task. For rapid screening, a simple platform that introduces a protease-specific probe into living cells is preferred. Our laboratory has previously generated a programmable protein module for the in vivo monitoring of HIV-1 Pr activity based on fluorescence resonance energy transfer (FRET) using HeLa cells transfected with the HIV proviral plasmid pNL4-3.HSA.R-E- (Biswas et al., 2011). Cleavage of the protein probes results in changes in FRET, which can be used to indicate the intracellular protease activity.

Correspondence to: W. Chen

Contract grant sponsor: NSF

Contract grant number: CBET1129012

Received 20 November 2013; Revision received 9 January 2014; Accepted 21 January 2014

Accepted manuscript online 29 January 2013;

Article first published online 21 February 2014 in Wiley Online Library

(<http://onlinelibrary.wiley.com/doi/10.1002/bit.25199/abstract>).

DOI 10.1002/bit.25199

In this work, we have extended the applicability of this cell-based assay to address the major hurdle in PI-based HIV therapy—resistance due to multiple mutations within the protease and the cleavage sites (Ali et al., 2010; Menéndez-Arias, 2010; Wensing et al., 2010). The ability to rapidly survey new PIs that are effective against these new variants is of great practical interest. The modular design of our method obviates the need for major redesign when targeting a new protease mutant or cleavage sequence, making this an ideal platform for identifying new PIs for drug-resistant HIV variants. In this paper, we demonstrate the feasibility of this approach by quantifying the in vivo cleavage rates of three known protease and cleavage site combinations in the presence or absence of different PIs. These mutations are widespread among patients undergoing HIV therapy and are identified as leading candidates to drug resistance by altering the hydrolysis rate of HIV-1 Pr.

Materials and Methods

Materials

TOPO capped Qdot[®] 545 ITK[™] Organic Quantum Dots (Qdot 545), Alexa Fluor[®] 568 C5 maleimide (Alexa 568) and Tris-(2-carboxyethyl) phosphine (TCEP) were purchased from Life Technologies. Dihydro lipoic acid (DHLA) was purchased from Sigma–Aldrich. HeLa cells were obtained from American Type Culture Collection. Autoclavable minimum essential medium (MEM) was from Irvine Scientific. Cell culture grade NaHCO₃, HEPES, nonessential amino acids, penicillin, and streptomycin L-glutamine was purchased from HyClone, Thermo Scientific. Fetal bovine serum (FBS) was purchased from Sigma–Aldrich. Restriction enzyme, ligase and polymerase enzymes were obtained from New England Biolabs (NEB).

Plasmid Construction and Protein Expression

The pET-H-MA/CA-ET expression vector coding for H-MA-ET was used (Biswas et al., 2011). To generate the NC-p1 cleavage site protein module, two overlapping oligos were ordered from Integrated DNA Technologies (IDT) with sequences CAT GGG CCA TCA CCA TCA CCA TCA CAC CGA ACG CCA GGC GAA CTT TCT GGG CAA AAT TTG GCC GTG CCA and TAT GGC ACG GCC AAA TTT TGC CCA GAA AGT TCG CCT GGC GTT CGG TGT GAT GGT GAT GGT GAT GGC C. The two oligos were mixed at equimolar concentrations and annealed together by heating to 95°C for 5 min and cooling gradually. The MA-CA fragment was removed by digesting pET-H-MA/CA-ET with *Nde*I and *Nco*I and the annealed DNA fragment was similarly digested and ligated overnight to obtain pET-H-NC/p1 WT-ET. A similar procedure was followed to obtain the mutant cleavage site variants using oligos CAT GGG CCA TCA CCA TCA CCA TCA CAC CGA ACG CCA GGT GAA CTT TCT GGG CAA AAT TTG GCC GTG CCA and TAT GGC ACG

GCC AAA TTT TGC CCA GAA AGT TCA CCT GGC GTT CGG TGT GAT GGT GAT GGT GAT GGC C, resulting in plasmid pET-H-NC/p1 M2-ET. Protein expression and purification by repeated thermal cycles were carried out similar to our previous report using *Escherichia coli* BL-21 (DE3) (Novagen, Madison, WI) as the host (Biswas et al., 2011). The protein purity was confirmed through SDS–PAGE gel electrophoresis and the protein concentration was determined by measuring the absorption at 215 nm.

To generate the protease mutant, the protease region (PR) of the pNL4-3.HSA.R-E- was amplified by using primers: PR-*Eco*RI/*Sph*I Forward: 5' AGTGAATTCGCATGCAGG-GCCTATTGCACC 3' and PR-*Xba*I/*Age*I Reverse: 5' TCTA-GACCGGTTCTTTTAGAATCTCCC 3'. The amplified product was digested with *Eco*RI and *Xba*I and cloned into corresponding restriction sites of pBlueScript –SK+ (Stratagene, La Jolla, CA) resulting in plasmid pBSK-PR. The protease mutations identified were introduced into pBSK-PR using the Quickchange Site-Directed Mutagenesis Kit (Stratagene) using the manufacturer's instructions. Primers for mutagenesis were ordered from Integrated DNA Technologies (IDT). Primers V82A Forward: 5'-tattagtag-gactacactgccaacataattggaagaaatctg-3' and V82A Reverse 5'-cagtattagtaggacctacactgtcaacataattggaagaaatctgtt-3' were used for introducing the V82A mutation. Primers L90M Forward 5'-cataattggaagaaatctgatgactcagattggctgcac-3' and L90M Reverse 5'-caacataattggaagaaatctgttactcagattggctg-cacttt-3' were used for introducing the L90M mutation. The mutated DNA fragments were digested with *Sph*I and *Age*I and ligated back into the pNL4-3.HSA.R-E- digested with the same enzymes. The mutations were confirmed by sequencing and large scale DNA preparation of the mutants, pNL4-3-V82A and pNL4-3-L90M, was performed using the Qiagen Maxi Prep Kit.

Alexa Labeling of Protein Modules

The labeling of proteins with Alexa Fluor[®] 568 C5 maleimide (Life Technologies) and the labeling efficiency determination was carried out as per the vendor instructions. Purified proteins were resuspended in 50 mM potassium phosphate buffer (pH 7) at a final concentration of 200 μM along with 10-fold excess TCEP in a final volume of 1,000 μL. The solution was incubated at room temperature on a rotator for 6 h and 10-fold excess Alexa 568 maleimide was added followed by incubation at room temperature for 2 h on a rotator. The solution was then transferred to a 4°C refrigerated rotator and incubated for 16 h. At the end of incubation period the unreacted dyes were removed by two thermal precipitation cycles. The degree of labeling was estimated by

$$\frac{A_x}{E} \times \frac{\text{Mol Wt of the protein}}{\text{mg protien/mL}} = \frac{\text{Moles of dye}}{\text{Moles of protien}}$$

where A_x is the absorbance value of the dye at 568 nm and E is the molar extinction coefficient of 92,000 cm⁻¹ M⁻¹.

Conjugation of Alexa-Label Protein Modules to Quantum Dot and FRET Analysis

Conjugation of Qdot[®] 545 ITK[™] Organic Quantum Dots (Life Technologies) to the Alexa-labeled proteins was carried out in HEPES (pH 8) buffer overnight at room temperature. The TOPO-capped CdSe/ZnS QD 545 obtained in decane are initially flocculated and resuspended in toluene as per manufacturer's instructions followed by water solubilization by exchanging the TOPO cap with DHLA. 300 nM of DHLA-capped QDs were mixed with the required molar ratio of Alexa-labeled proteins, resuspended in 10 mM HEPES buffer (pH 8.2), and incubated at room temperature on a rotator for 12 h. The conjugation was confirmed by measuring the FRET efficiency using a fluorometer by exciting at 430 nm and recording the spectrum from 500 to 700 nm.

Intracellular Probe Delivery and Inhibitor Evaluation

HeLa cells were cultured in T-50 flasks using 1× minimum essential medium (Gibco) at 37°C and 5% CO₂. HIV infection and production of the HIV protease is achieved through a plasmid system (pNL4-3.HSA.R-E-) with sequence of wild-type HIV-1 strain (HXB2). The probe delivery and transfection with the proviral vector was done similar to previously reported (Biswas et al., 2011). Cell imaging was performed with a Axio observer z1 motorized inverted microscope (Zeiss). The objective used was LD Plan-Neofluar 20×/0.4Ph2CorrWD = 8.4M27 from Zeiss. Fluorescent probes were detected by using two different filter sets; QD filter consisting of a D436-nm exciter, a D535/50-nm emitter, and a 475 nm-dichroic long pass beam splitter (Chroma Technology) and FRET filter consisting of ET450/50×, ET595/40 m and T495LPXR, 25 mm diameter excitation and emission filters, 25.5 × 36 mm² dichroic. Images were acquired by using the Axio-vision software from Zeiss and fluorescence images were analyzed by using Image-Pro PLUS analysis software (Media Cybernetics).

For the inhibitor experiments, cells after probe delivery were incubated with growth media containing respective concentrations of PIs for 4 h following which transfection was carried out. After transfection, the replaced growth media also contained PIs at required concentrations. The percentage inhibition efficiency was calculated from the quantified FRET/Qdot values for three random regions according to the equation:

$$\begin{aligned} \% \text{ Inhibition efficiency} \\ = \frac{\text{FRET ratio}_{\text{inhibitor}} - \text{FRET ratio}_{\text{no inhibitor}}}{\text{FRET ratio}_{\text{control}} - \text{FRET ratio}_{\text{no inhibitor}}} \end{aligned}$$

Results and Discussion

Probe Design and FRET Characterizations

The probe design is illustrated in Figure 1 (Biswas et al., 2011). The N-terminus contains a hexahistidine tag that is used to conjugate to the QD surface through metal affinity

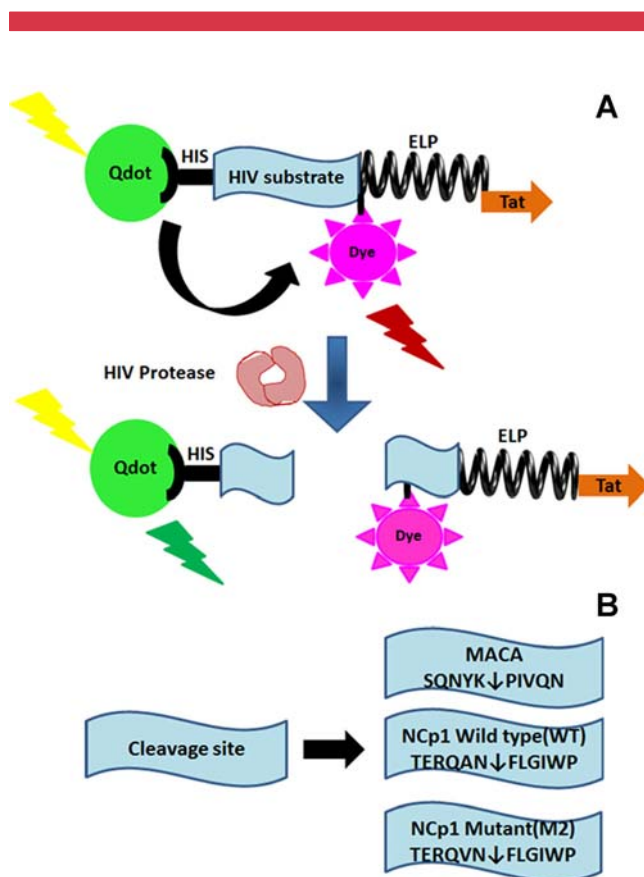


Figure 1. Protein probes employed in this work. **A:** Presence of active HIV-1 Pr disrupts FRET resulting in an increase in the QD emission and a corresponding decrease in the Alexa emission. **B:** The different cleavage sequences employed in this work.

interactions. Incorporation of an elastin like polypeptide (ELP) domain facilitates purification by reversible thermal precipitation (Kim et al., 2005). A unique cysteine residue is incorporated between the cleavage sequence and the ELP domain for conjugation of Alexa dyes through thiol maleimide reaction. This alexa dye acts as fluorescence acceptor. Finally, a tat peptide sequence is inserted for intracellular delivery (Brooks et al., 2005). In the presence of HIV-1 Pr, the probe is cleaved and the QD and Alexa dye are separated resulting in the disruption of FRET.

The protein module (H-MA-ET) containing the MA/CA cleavage sequence was purified and labeled with Alexa 568 as reported previously (Biswas et al., 2011), and subsequently conjugated to DHLA-capped CdSe–ZnS QDs (QD₅₄₅) because of the favorable spectral overlap with Alexa 568. Successful conjugation was first confirmed by agarose gel analysis and a clear shift in the QD mobility was detected (Fig. 2C). Assembling an increasing number of labeled H-MA-ET (*n*) onto the QDs reduced their emission, while a corresponding increase in the Alexa emission was observed (Fig. 2A). By analyzing the QD-protein complexes by SDS-PAGE, we demonstrated that virtually all added H-MA-ET proteins were conjugated to QDs with *n* up to 40 as very little

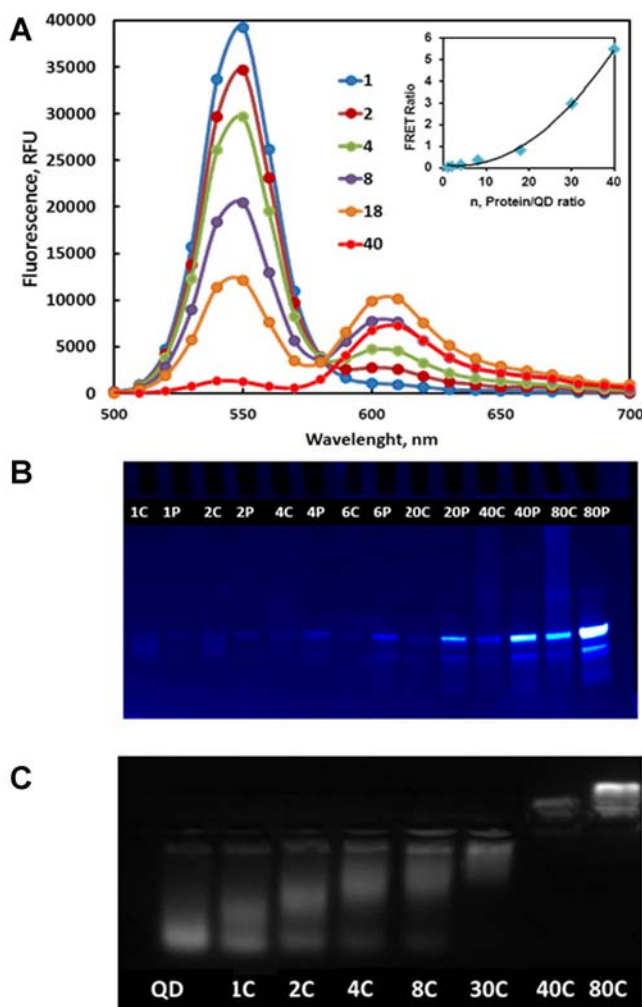


Figure 2. Characterization of QD-Alexa-labeled H-MA-ET conjugation. **A:** Fluorescence spectra obtained by conjugating an increasing number of labeled H-MA-ET to QD. The resulting FRET (Alexa/QD) ratio is shown in the inset. **B:** SDS-PAGE analysis of protein-QD complexes (C) and the unconjugated Alexa-labeled H-MA-ET (P). Only unconjugated proteins migrated into the gel and detected under UV light. **C:** Confirmation of QD conjugation with Alexa-labeled H-MA-ET at different ratios (*n*) through changes in migration pattern of the conjugates in a 1% agarose gel.

unconjugated proteins were detected (Fig. 2B). Because the FRET (Alexa/QD) ratio is well correlated with the number of Alexa-labeled H-MA-ET per QD, changes in the FRET ratio can be used to reflect the number of conjugated proteins removed because of protease cleavage.

In Vivo FRET Characterization and Probe Cleavage

To test whether we can capture a similar change in the FRET ratio in vivo, different protein-QD conjugates were delivered into HeLa cells (Fig. S1). Fluorescence images captured were quantified and expressed as the whole-cell FRET ratio using image analysis tools. Similar to the in vitro results, a gradual increase in the in vivo FRET ratio was detected when the number of labeled H-MA-ET per QD was increased. By

estimating the intracellular protein concentrations based on the probe concentration, the number of cells per well, and the average volume of HeLa cell at confluency, a correlation between the in vivo FRET ratio and the concentration of intact protein per QD was established (Fig. 3A). This serves as the standard curve for calculating the cleavage of intact H-MA-ET for in vivo experiments.

To quantify the in vivo cleavage, probes with an H-MA-ET to QD ratio of 40 were delivered to HeLa cells. Following transfection with the HIV proviral plasmid pNL4-3.HSA.R-E-, fluorescent images for the untransfected and the transfected cells were captured temporally under a fluorescence microscope (Fig. S3). While the fluorescence signal remained unchanged for untransfected cells, a gradual shift toward the QD fluorescence was detected for the transfected samples due to probe cleavage by HIV-1 Pr (Fig. 3C). In

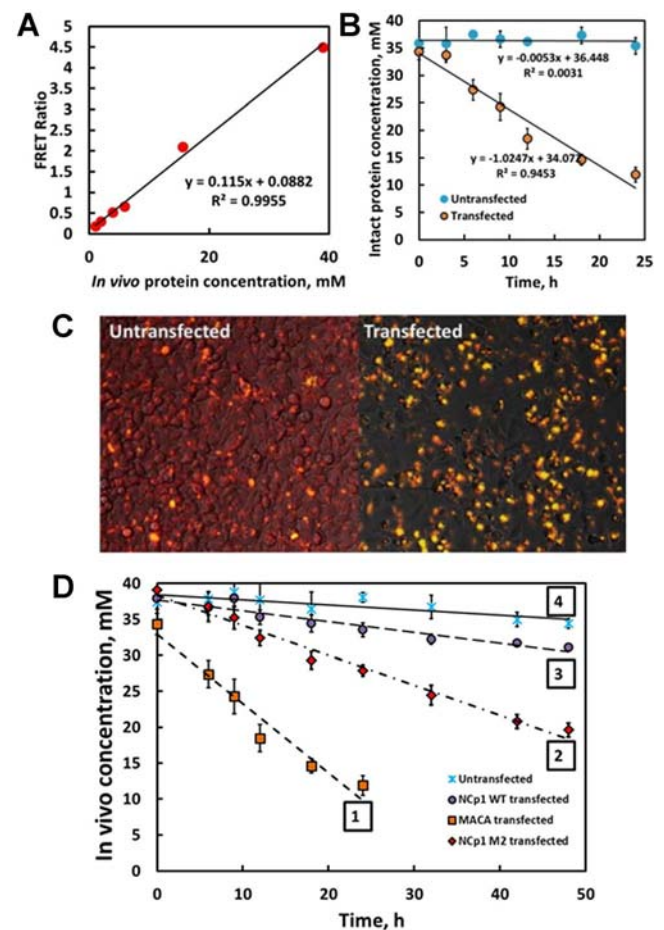


Figure 3. In vivo characterization of QD-conjugated probes. **A:** A calibration plot correlating the whole-cell FRET ratio to the in vivo protein concentration. **B:** Cleavage of intracellular QD probes (H-MA-ET) by HIV-1 Pr. **C:** In vivo cleavage of H-MA-ET probes. The composite merged DIC, QD, and Alexa images are shown for transfected or untransfected cells. **D:** Changes in the intact probe concentration with time of (1) H-MA-ET conjugate, (2) H-NC-WT-ET conjugate, (3) H-NC-M2 conjugate, and (4) probe in untransfected wells. The measurements are average of three independent experiments.

contrast, the fluorescence signal for a similar probe containing the West Nile Virus (WNV) protease cleavage sequence (H-WNV-ET) remained unchanged even for transfected cells, validating the specificity of the approach (Fig. S3). The fluorescence images were quantified and used to determine the intact probe concentrations and the corresponding in vivo cleavage rate (Fig. 3B).

Quantitative Analysis of In Vivo Probe Cleavage

Since the intracellular probe concentration of 38 nM is far in excess of the reported K_m of all the cleavage sites (Cheng et al., 1990; Feher et al., 2002; Tözsér et al., 1991), the in vivo cleavage rate can be used to compare the k_{cat} value of different target sequences. To test this feasibility, a new protein module containing the NC/p1 cleavage sequence (H-NC-WT-ET; Fig. 1), which has a reported 20-fold lower k_{cat} value compared to the MA/CA site, was generated (Maschera et al., 1996). A similar calibration curve for the whole-cell FRET ratio was obtained as described above (data not shown). Intracellular cleavage experiments were conducted and the in vivo cleavage rate was determined (Fig. 3D, trace 3). The calculated rate of 22 nM/s for H-NC-WT-ET is roughly 13-fold lower than that observed using the MA/CA sequence (284 nM/s), consistent with the reported difference in k_{cat} (Feher et al., 2002). This result confirms the ability of our method to quantitatively assess the in vivo cleavage rate of different target sequences. Because the NC/p1 site is the rate-limiting step in HIV polyprotein processing, it is the most frequently mutated cleavage site found in parallel with protease mutations in drug-resistant HIV variants (Bally et al., 2000; Wondrack et al., 1993). Mutations at this site act to compensate the loss of viral fitness by increasing the catalytic efficiency. To demonstrate that our assay is useful for screening PIs for drug-resistant HIV variants, a new protein module (H-NC-M2-ET) containing a commonly detected mutation (A431V) in NC/p1 was constructed (Fig. 1). The QD probes were delivered into HeLa cells and fluorescence changes were captured. The calculated hydrolysis rate for this probe was fourfold higher compared to the wild-type Nc/p1 (trace 2, Fig. 3C) in accordance with the reported differences in the k_{cat} value (Feher et al., 2002).

Drug Screening Using a Combination of Cleavage Site and Protease Mutations

To further demonstrate the versatility of our system, we incorporated two separate point mutations into the protease region of the proviral vector, pNL4-3.HSA.R-E- (HXB2). Both mutations are known to be associated with the NC-p1 cleavage site mutation (A431V) in many drug-resistant HIV variants (Nijhuis et al., 2006; Zhang et al., 1997). Viruses with the V82A mutation are known to be highly resistant to one particular PI Indinavir with a reported 20-fold increase in the IC_{50} value (Kolli et al., 2009). The L90M mutation, on the other hand, confers resistant to all PIs and is one of the few known mutations to provide more than a 10-fold change in

the IC_{50} value for Saquinavir (Kolli et al., 2009). These two mutations were introduced separately into the protease region by site directed mutagenesis (Fig. 4A), and the functionality of the two mutant proteases was first confirmed by detecting the in vivo cleavage of the MA/CA probes. The wild-type protease (HXB2) and the two mutants (V82A and L90M) hydrolyzed the MACA substrate with similar rates (Fig. S4) indicating that the two mutants remained functional upon transfection. To verify that our assay can effectively capture the decrease in PI efficacy, in vivo cleavage experiments were conducted in the presence of increasing concentrations of the two PIs—Indinavir and Saquinavir using either the wild-type or mutant protease in combination with the mutant H-NC-M2-ET probe. By quantifying the in vivo cleavage rates, a marked difference in the inhibition efficacy was detected between the wild type and mutant proteases (Fig. 4B). The calculated IC_{50} values for the wild-type protease are in accordance with the literature reports (Kolli et al., 2009). More importantly, both protease mutants were shown to significantly impair the inhibition efficiency (Table I), indicating that our reported assay is suitable in evaluating the in vivo efficacy of different PIs in the presence of a combination of cleavage site and protease mutations.

In summary, we reported here a highly modular assay for the in vivo evaluation of HIV-1 Pr activity. Because of the ease of introducing mutations into both the HIV-1 protease and the cleavage sites, the reported QD-based assay is ideal for the

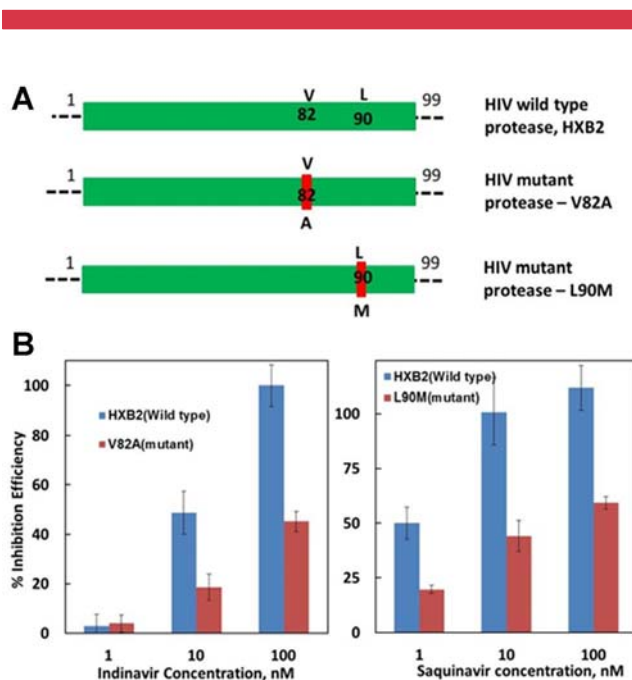


Figure 4. In vivo assessment of inhibitor efficiency using a combination of cleavage site and protease mutants. **A:** The wild-type (HXB2) and mutant (V82A and L90M) HIV-1 proteases employed in the study. **B:** The in vivo inhibition efficiency of Indinavir or Saquinavir against either the wild-type or mutant protease using the H-NC-M2-ET probe.

Table I. The reported and measured IC₅₀ values for the different protease and cleavage site mutations.

	Reported IC ₅₀	Measured IC ₅₀
HXB2 + Indinavir	20 nM	10 nM
V82A + Indinavir	10–20-fold increase	>10-fold increase
HXB2 + Saquinavir	5 nM	5 nM
L90M + Saquinavir	4–10-fold increase	10-fold increase

expedited discovery of new PIs against drug-resistant HIV variants.

This work was supported by a grant from NSF (CBET1129012).

References

- Ali A, Bandaranayake RM, Cai Y, King NM, Kolli M, Mittal S, Murzycki JF, Nalam MNL, Nalivaika EA, Özen A, Prabu-Jeyabalan MM, Thayer K, Schiffer CA. 2010. Molecular basis for drug resistance in HIV-1 protease. *Viruses* 2:2509–2535.
- Bally F, Martinez R, Peters S, Sudre P, Telenti A. 2000. Polymorphism of HIV type 1 gag p7/p1 and p1/p6 cleavage sites: Clinical significance and implications for resistance to protease inhibitors. *AIDS Res Hum Retroviruses* 16:1209–1213.
- Biswas P, Cella LN, Kang SH, Mulchandani A, Yates MV, Chen W. 2011. A quantum-dot based protein module for in vivo monitoring of protease activity through fluorescence resonance energy transfer. *Chem Commun (Camb)* 47:5259–5261.
- Brik A, Wong C. 2003. HIV-1 protease: Mechanism and drug discovery. *Org Biomol Chem* 1:5–14.
- Brooks H, Lebleu B, Vivès E. 2005. Tat peptide-mediated cellular delivery: Back to basics. *Adv Drug Deliv Rev* 57:559–577.
- Cheng YS, Yin FH, Foundling S, Blomstrom D, Kettner CA. 1990. Stability and activity of human immunodeficiency virus protease: Comparison of the natural dimer with a homologous, single-chain tethered dimer. *Proc Natl Acad Sci USA* 87:9660–9664.
- Cheng Y-SE, Lo K-H, Hsu H-H, Shao Y-M, Yang W-B, Lin C-H, Wong C-H. 2006. Screening for [HIV] protease inhibitors by protection against activity-mediated cytotoxicity in *Escherichia coli*. *J Virol Methods* 137: 82–87.
- Craig JC, Duncan IB, Hockley D, Grief C, Roberts NA, Mills JS. 1991. Antiviral properties of Ro 31-8959, an inhibitor of human immunodeficiency virus (HIV) proteinase. *Antivir Res* 16:295–305.
- Dayam R, Neamati N. 2003. Small-molecule HIV-1 integrase inhibitors: The 2001–2002 update. *Curr Pharm Des* 9:1789–1802.
- De Clercq E. 2002. Strategies in the design of antiviral drugs. *Nat Rev Drug Discov* 1:13–25.
- Feher A, Weber IT, Bagossi P, Boross P, Mahalingam B, Louis JM, Copeland TD, Torshin IY, Harrison RW, Tozser J. 2002. Effect of sequence polymorphism and drug resistance on two HIV-1 Gag processing sites. *Eur J Biochem* 269:4114–4120.
- Fuse T, Watanabe K, Kitazato K, Kobayashi N. 2006. Establishment of a new cell line inducibly expressing HIV-1 protease for performing safe and highly sensitive screening of [HIV] protease inhibitors. *Microbes Infect* 8:1783–1789.
- Grabar S, Pradier C, Le Corfec E, Lancar R, Allavena C, Bentata M, Berlureau P, Dupont C, Fabbro-Peray P, Poizot-Martin I, Costagliola D. 2000. Factors associated with clinical and virological failure in patients receiving a triple therapy including a protease inhibitor. *AIDS* 14:141–149.
- Imamichi T. 2004. Action of anti-HIV drugs and resistance: Reverse transcriptase inhibitors and protease inhibitors. *Curr Pharm Des* 10:4039–4053.

- Kim J-Y, Mulchandani A, Chen W. 2005. Temperature-triggered purification of antibodies. *Biotechnol Bioeng* 90:373–379.
- Kolli M, Stawiski E, Chappey C, Schiffer CA. 2009. Human immunodeficiency virus type 1 protease-correlated cleavage site mutations enhance inhibitor resistance. *J Virol* 83:11027–11042.
- Maschera B, Darby G, Palu G, Wright LL, Tisdale M, Myers R, Blair ED, Furfine ES. 1996. Mutations in the viral protease that confer resistance to saquinavir increase the dissociation rate constant of the protease-saquinavir complex. *J Biol Chem* 271:33231–33235.
- Menéndez-Arias L. 2010. Molecular basis of human immunodeficiency virus drug resistance: An update. *Antiviral Res* 85:210–231.
- Navia MA, Fitzgerald PM, McKeever BM, Leu CT, Heimbach JC, Herber WK, Sigal IS, Darke PL, Springer JP. 1989. Three-dimensional structure of aspartyl protease from human immunodeficiency virus HIV-1. *Nature* 337:615–620.
- Nijhuis M, van Maarseveen NM, de Jong D, Schipper PJ, Goedegebuure IW, Boucher CAB. 2006. Substitutions within Gag but outside the cleavage sites can cause protease inhibitor resistance. *Antivir Ther* 11: S149.
- Randolph JT, DeGoeys DA. 2004. Peptidomimetic inhibitors of HIV protease. *Curr Top Med Chem* 4:1079–1095.
- Robinson BS, Riccardi KA, Gong YF, Guo Q, Stock DA, Blair WS, Terry BJ, Deminie CA, Djang F, Colonna RJ, Lin PF. 2000. BMS-232632, a highly potent human immunodeficiency virus protease inhibitor that can be used in combination with other available antiretroviral agents. *Antimicrob Agents Chemother* 44:2093–2099.
- Roh C, Lee H-Y, Kim S-E, Jo S-K. 2010. A highly sensitive and selective viral protein detection method based on RNA oligonucleotide nanoparticle. *Int J Nanomedicine* 5:323–329.
- Sham HL, Kempf DJ, Molla A, Marsh KC, Kumar GN, Chen CM, Kati W, Stewart K, Lal R, Hsu A, Betebenner D, Korneyeva M, Vasavanonda S, McDonald E, Saldivar A, Wideburg N, Chen X, Niu P, Park C, Jayanti V, Grabowski B, Granneman GR, Sun E, Japour AJ, Leonard JM, Plattner JJ, Norbeck DW. 1998. ABT-378, a highly potent inhibitor of the human immunodeficiency virus protease. *Antimicrob Agents Chemother* 42:3218–3224.
- Tözsér J, Bláha I, Copeland TD, Wondrack EM, Oroszlan S. 1991. Comparison of the HIV-1 and HIV-2 proteinases using oligopeptide substrates representing cleavage sites in Gag and Gag-Pol polyproteins. *FEBS Lett* 281:77–80.
- UNAIDS. 2010. UNAIDS Report on the global HIV/AIDS epidemic.
- Vacca JP, Dorsey BD, Schleif WA, Levin RB, McDaniel SL, Darke PL, Zugay J, Quintero JC, Blahy OM, Roth E. 1994. L-735,524: An orally bioavailable human immunodeficiency virus type 1 protease inhibitor. *Proc Natl Acad Sci USA* 91:4096–4100.
- Virgil SC. 2010. First-generation HIV-1 protease inhibitors for the treatment of HIV/AIDS. In: Ghosh AK, editor. Aspartic acid proteases as therapeutic targets. Weinheim, Germany: Wiley-VCH Verlag GmbH & Co. KGaA. p 139–168.
- Wensing AMJ, van Maarseveen NM, Nijhuis M. 2010. Fifteen years of [HIV] protease inhibitors: Raising the barrier to resistance. *Antiviral Res* 85:59–74.
- Wondrack EM, Louis JM, Derocquigny H, Chermann JC, Roques BP. 1993. The gag precursor contains a specific HIV-1 protease cleavage site between the NC (P7) and p1 proteins. *FEBS Lett* 333:21–24.
- Zhang YM, Imamichi H, Imamichi T, Lane HC, Falloon J, Vasudevachari MB, Salzman NP. 1997. Drug resistance during indinavir therapy is caused by mutations in the protease gene and in its Gag substrate cleavage sites. *J Virol* 71:6662–6670.

Supporting Information

Additional supporting information may be found in the online version of this article at the publisher's web-site.